INTERNATIONAL JOURNAL FOR NUMERICAL METHODS IN ENGINEERING, VOL. 36, 3057–3066 (1993)

LINKED INTERPOLATION FOR REISSNER–MINDLIN PLATE ELEMENTS: PART II—A SIMPLE TRIANGLE

ROBERT L. TAYLOR AND FERDINANDO AURICCHIO

Department of Civil Engineering, University of California at Berkeley, CA 94720, U.S.A.

SUMMARY

The formulation and shape functions given in Part I are extended to develop a simple plate bending triangle with good performance in both thin and thick situations. Indeed, its performance is better than that of other nine DOF elements and its computer implementation simpler. When used with selective reduced integration, the element produces identical results as that of Xu.[1,2] To save space, details given in Part I are not repeated and some results are also presented in the figures of Part I.

1. INTRODUCTION

In the present paper we develop and study a simple triangular element for the Reissner–Mindlin plate theory using the mixed formulation described in Part I, Section 2.[1]

In the development of a mixed finite element for thick plate theory, the transverse displacement w, the rotations θ and the transverse shear S are usually interpolated independently of each other:

$$w = \mathbf{N}_w \bar{\mathbf{w}} \tag{1}$$

$$\boldsymbol{\theta} = \mathbf{N}_\theta \bar{\boldsymbol{\theta}} \tag{2}$$

$$\mathbf{S} = \mathbf{N}_s \bar{\mathbf{S}} \tag{3}$$

where $\bar{\mathbf{w}}$, $\bar{\boldsymbol{\theta}}$, $\bar{\mathbf{S}}$ are the degrees of freedom of the discretized system and $\mathbf{N}_w$, $\mathbf{N}_\theta$, $\mathbf{N}_s$ are the corresponding shape functions.

As in Part I, we show that better performance results if the interpolation for the transverse displacement field is of the form

$$w = \mathbf{N}_w \bar{\mathbf{w}} + \mathbf{N}_{w\theta}\, \bar{\boldsymbol{\theta}} \tag{4}$$

The element derived gives identical results as the one presented by Xu[2,3] when reduced integration is selectively used, but the derivation given here is much simpler.

2. THE NEW TRIANGULAR ELEMENT (T3L)

The element parameters chosen are those shown in Figure 1 and include internal 'nodes' for θ and S variables.

The essential functions to satisfy the patch test are the linear interpolations

$$N_\theta^i = N_w^i = L_i \quad i = 1\text{–}3 \tag{5}$$

where L_i is the appropriate area co-ordinate.[4,5]

0029–5981/93/183057–10$10.00

Received 18 February 1993
Revised 18 February 1993

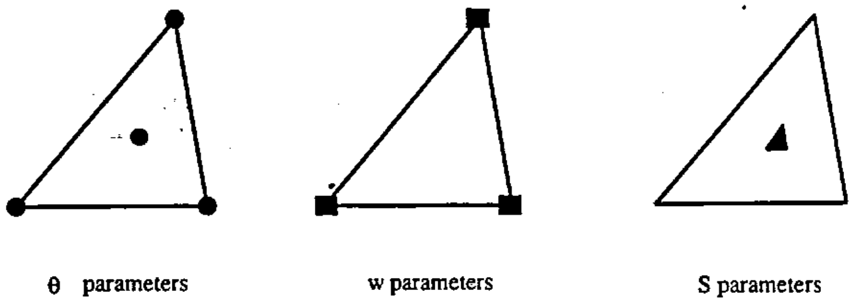

Figure 1. A linear triangular mixed element

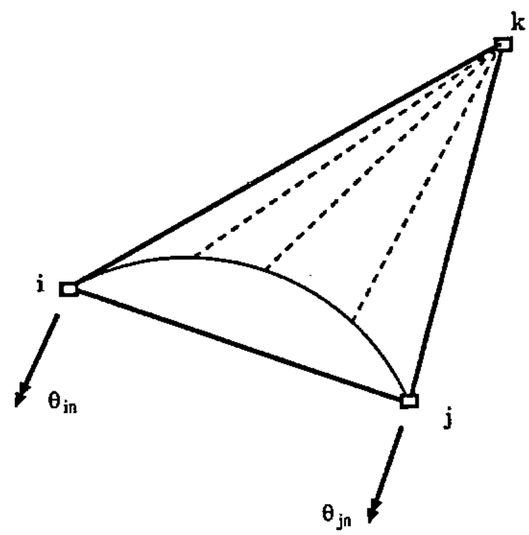

Figure 2. Design of linking shape functions $N_{w\theta}$

For the internal node 4, a hierarchical bubble function in the form

$$N_\theta^4 = 27\, L_1 L_2 L_3 \tag{6}$$

is chosen and for the shears a constant value is again assumed, with

$$N_s = 1 \tag{7}$$

The additional shape function $N_{w\theta}$ are derived in an identical manner to that described in Part I from side components as

$$N_{w\theta}^{12} = L_1 L_2 (\theta_{12}^2 - \theta_{12}^1) h_{12}/2 \tag{8}$$

where h_{12} is the length of side 12.

The factor 1/2 has been chosen in a similar manner to the α of equation (17) of Part I to ensure constant shears and Figure 2 shows this shape function graphically.

Once again, projection along x and y co-ordinates gives the shape functions referring to global axes of form identical to equation (18) of Part I, i.e.

$$N^1_{w\theta} = \begin{bmatrix} x_1 & -x_3 \\ y_1 & -y_3 \end{bmatrix} N^{31}_{w\theta} + \begin{bmatrix} x_1 & -x_2 \\ y_1 & y_2 \end{bmatrix} N^{12}_{w\theta} \quad (9)$$

with a cyclic permutation 1–2–3, etc. The remainder of the evaluation of stiffness matrices, etc., follows an identical pattern to the one previously presented. However, in the present element we also investigate a simple point quadrature for matrices $\hat{C}$ and E defined in Part I. The element using full integration will be referred to as T3BL and with the selective reduced integration as T3BL(R). For full integration seven-point quadrature was used as given in References 4 and 6.

3. NUMERICAL PERFORMANCE

The performance of the element discussed in the previous section was checked on several numerical tests. The elements was implemented into the finite element analysis program (FEAP)[4,5] and this environment was used for all the computations.

Where no analytical or series solution of the problem is available, the numerical solution was compared with that obtained using the Q4BL element described in Part I[1] and/or with that obtained from the DRM element.[7]

The test problems are organized in the following order:

- patch test, stability assessment,
- patch test, consistency assessment,
- square plate,
- circular plate,
- skew cantilever plate,
- simply supported skew plate.

Only uniform loading is considered, since the transverse displacement for a concentrated load is infinite for a theory which includes the effects of shear deformation; moreover, the load is computed consistently using the transverse displacement shape functions.

3.1. Patch test: stability assessment

As described in Reference 5 and in equation (10) of Part I, Section 2, the mesh for any patch must satisfy two constraint requirements:

$$n_\theta + n_w \geqslant n_s, \quad n_s \geqslant n_w$$

These algebraic requirements were checked both on a single-element mesh (either with all the boundaries fixed or with a minimum number of degrees of freedom restrained to prevent rigid body modes) and on a regular square mesh of the type used later for square plates. Recalling that S is a constant in each element, the count reduces to comparing n_s with n_w; the other condition is always satisfied since θ has two internal modes which exactly balance n_s. For the meshes discussed, the algebraic constraint count is always satisfied by the triangular element described here.

Although the constraint count is a necessary condition, it is still not sufficient to guarantee the stability of a particular element. To assess actual performance of our formulation, an eigen-analysis on the stiffness matrix for patches of one or more elements is performed. Both versions of the element fail the eigen-analysis test for a single element since they show one extra zero-energy mode, but repeating the eigen-analysis using two or more elements results in no spurious modes. Thus, we can assert that in real applications the triangular element is stable provided sufficiently boundary conditions are imposed to prevent rigid body motions.

3.2. Patch test: consistency assessment

A patch test to assess the consistency of the formulation was conducted on a square plate of arbitrary triangles as in References 5 and 7. In terms of load and displacement the following boundary conditions were considered:

- pure bending—distributed constant edge moment along one edge, the opposite edge is clamped and all lateral boundary tangential rotations are fixed;
- pure twist—distributed constant edge twisting moments along all four sides, three corner nodes are restrained to prevent rigid body motion;
- pure shear—distributed constant edge forces on one edge, the opposite edge is clamped, and all rotations fixed in order to prevent bending.

The second part of the consistency assessment test is based on a set of problems which approach the limiting case of a thin plate. For a one-element mesh the ratio between the thickness t and the side length L is varied between 10 and 10^5; Young's modulus is also varied in order to maintain a constant value of the bending stiffness D. Consequently, the modes in the element associated with bending effects remain approximately constant, while those influenced by the shear increase by $(L/t)^2$. This test can be useful for checking the tendency of an element to lock; it also indicates whether all modes included in each interpolation are available in the actual solution process. Finally, it may allow an assessment of whether any of the eigenvalues tends to zero in the limiting case of thin plates.

The element passed both the above consistency tests.

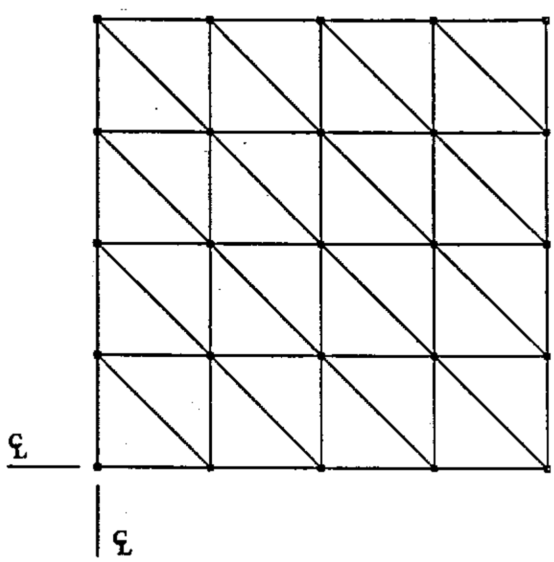

Figure 3. Typical mesh (4 × 4) for the square plate problem

3.3. *Square plate*

A square plate is modelled using meshes of the type presented in Figure 3. Two simply supported boundary conditions are considered: *soft* (SS1) and *hard* (SS2); a discussion of these boundary conditions is given in Part I of this paper and in References 5 and 6. A clamped plate is also considered.

The results are presented in Tables I and II in the same manner as in Part I but now considering the differently integrated forms T3BL and T3BL(R).

The series solutions reported were evaluated for thick plates using only the SS2 (hard) boundary simple support since special difficulties arise with the soft SS1 condition.

Table I. Displacements and moments at the centre of the square plate (uniform load, simply supported boundary)

Mesh		$L/t = 10$ ($t = 1$)		$L/t = 1000$ ($t = 0{\cdot}01$)	
		$W_c\Big/\left(\frac{qL^4}{100D}\right)$	$-Mc\Big/\left(\frac{qL^2}{100}\right)$	$W_c\Big/\left(\frac{qL^4}{100D}\right)$	$-Mc\Big/\left(\frac{qL^2}{100}\right)$
T3BL					
2×2	(SS2)	0·403591	4·48351	0·377793	4·26461
($M = 2$)	(SS1)	0·412562	4·57061	0·379834	4·28487
4×4	(SS2)	0·421194	4·74389	0·399068	4·65804
($M = 4$)	(SS1)	0·438015	4·90195	0·400505	4·67219
8×8	(SS2)	0·425688	4·78521	0·404642	4·76074
($M = 8$)	(SS1)	0·451866	5·02310	0·405383	4·76747
16×16	(SS2)	0·426869	4·78940	0·405871	4·78282
($M = 16$)	(SS1)	0·458561	5·07377	0·406306	4·78673
32×32	(SS2)	0·427177	4·78915	0·406150	4·78747
($M = 32$)	(SS1)	0·460839	5·09002	0·406408	4·78978
64×64	(SS2)	0·427257	4·78883	0·406216	4·78844
($M = 64$)	(SS1)	0·461472	5·09432	0·406381	4·78991
T3BL(R)					
2×2	(SS2)	0·431926	4·54513	0·413703	4·53305
($M = 2$)	(SS1)	0·449645	4·72021	0·425312	4·64723
4×4	(SS2)	0·428831	4·75141	0·408626	4·73888
($M = 4$)	(SS1)	0·450776	4·95696	0·416389	4·80842
8×8	(SS2)	0·427655	4·78585	0·406873	4·77946
($M = 8$)	(SS1)	0·455681	5·04001	0·411369	4·81947
16×16	(SS2)	0·427366	4·78945	0·406399	4·78715
($M = 16$)	(SS1)	0·459561	5·07817	0·408808	4·80853
32×32	(SS2)	0·427302	4·78915	0·406278	4·78847
($M = 32$)	(SS1)	0·461090	5·09112	0·407532	4·79959
64×64	(SS2)	0·427288	4·78883	0·406248	4·78865
($M = 64$)	(SS1)	0·461535	5·09459	0·406997	4·79450
Series soln (thick)	(SS2)	0·427284	4·78863	0·406237	4·78863
Series soln (thin)	both	0·406235	4·78863	0·406235	4·78863

Table II. Displacements and moments at the centre of the square plate (uniform load, clamped boundary)

Mesh		$L/t = 10$ ($t = 1$)		$L/t = 1000$ ($t = 0{\cdot}01$)	
		$W_c \Big/ \left(\frac{qL^4}{100D}\right)$	$-Mc \Big/ \left(\frac{qL^2}{100}\right)$	$W_c \Big/ \left(\frac{qL^4}{100D}\right)$	$-Mc \Big/ \left(\frac{qL^2}{100}\right)$
2×2	(T3BL)	0·126275	1·59649	0·093098	1·40767
($M = 2$)	T3BL(R)	0·169086	1·64715	0·144588	1·61736
4×4	(T3BL)	0·144973	2·15009	0·118006	2·10245
($M = 4$)	T3BL(R)	0·155232	2·15474	0·130768	2·12234
8×8	(T3BL)	0·149114	2·27741	0·124616	2·24825
($M = 8$)	T3BL(R)	0·151637	2·27854	0·127567	2·24853
16×16	(T3BL)	0·150131	2·30930	0·126092	2·28031
($M = 16$)	T3BL(R)	0·150757	2·30959	0·126792	2·27998
32×32	(T3BL)	0·150382	2·31734	0·126429	2·28798
($M = 32$)	T3BL(R)	0·150538	2·31741	0·126599	2·28787
64×64	(T3BL)	0·150443	2·31933	0·126509	2·28987
($M = 64$)	T3BL(R)	0·150482	2·31935	0·126551	2·28985
Thick (see part I)		0·1499	2·31	0·1265	2·29
Series soln (thin)		0·126532	2·2905	0·126532	2·2905

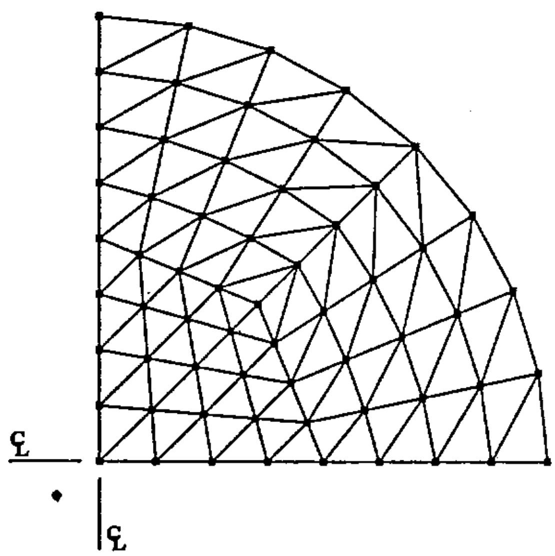

Figure 4. Circular plate—typical mesh of 96 elements

3.4. Circular plate

The geometry and details of this problem are as described in Section 4.2 of Part I. However, the set of meshes used is now different and generally of the form shown in Figure 4. The results are given in Table III.

Table III. Displacements and moments at the centre of the circular plate under a uniform load

	$R/t = 5$ $(t = 1)$				$R/t = 50$ $(t = 0{\cdot}1)$			
	SS1 boundary		Clamped boundary		SS1 boundary		Clamped boundary	
Mesh (NEL)	W_c	$-M_c$	W_c	$-M_c$	W_c	$-M_c$	W_c	$-M_c$
T3BL								
A (6)	41·1627	4·72366	8·03919	1·28848	39431·9	4·70841	6049·46	1·21883
B (24)	41·4296	5·02944	10·6006	1·82579	39657·6	5·03098	8774·99	1·81886
C (96)	41·5555	5·12392	11·3022	1·97800	39784·8	5·12424	9523·66	1·97714
D (384)	41·5891	5·14840	11·4774	2·01695	39820·0	5·14859	9708·70	2·01702
E (1536)	41·5971	5·15445	11·5207	2·02665	39828·7	5·15448	9753·53	2·02667
F (6144)	41·5989	5·15586	11·5478	2·03054	39830·8	5·15586	9784·74	2·03163
T3BL(R)								
A (6)	43·9038	4·74597	10·8377	1·32959	42215·8	4·74860	9119·24	1·33035
B (24)	42·2235	5·03419	11·4059	1·83157	40460·9	5·03804	9640·34	1·83543
C (96)	41·7594	5·12427	11·5066	1·97838	39943·4	5·12172	9738·15	1·97888
D (384)	41·6402	5·14843	11·5285	2·01698	39802·6	5·14363	9760·75	2·01705
E (1536)	41·6099	5·15445	11·5334	2·02665	39764·4	5·14884	9766·35	2·02666
F (6144)	41·6021	5·15586	11·5510	2·03054	39834·0	5·15586	9788·16	2·03167
Exact solution	41·5994	5·1563	11·5513	2·0313	39831·5	5·1563	9783·48	2·0313

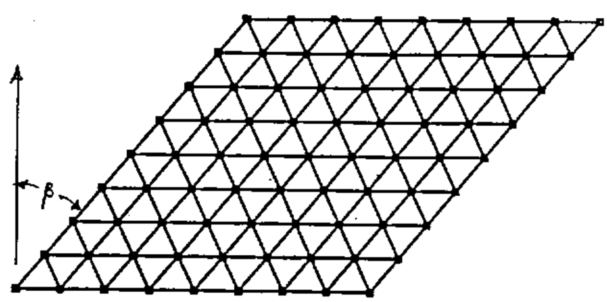

Figure 5. Skew cantilever plate 8 × 8 mesh $\beta = 40°$

3.5. *Skew cantilever*

Again the geometry and other data are given in Section 4.3 of Part I and the results are given in Table IV. Here mesh subdivisions of the regular type shown in Figure 5 were used.

3.6. *Simply supported (Morley) skew plate*

Once again, regular subdivisions similar to those shown in Figure 5 were used. Table V shows the results together those reported by Babuska and Scapolla[8] and the thin plate results of

Table IV. Displacements at the tips of the skew cantilever plate

	$\beta = 20°$		$\beta = 40°$		$\beta = 60°$	
Mesh	$w_A(Et^3/qL^4)$	$w_B(Et^3/qL^4)$	$w_A(Et^3/qL^4)$	$w_B(Et^3/qL^4)$	$w_A(Et^3/qL^4)$	$w_B(Et^3/qL^4)$
T3BL						
2 × 2	1·17926	0·96769	0·88110	0·452927	0·581632	0·100257
4 × 4	1·35210	1·02099	1·06333	0·516100	0·707712	0·130870
8 × 8	1·40800	1·03740	1·14222	0·537132	0·791187	0·146650
16 × 16	1·42377	1·04207	1·17215	0·544102	0·831366	0·153775
32 × 32	1·42892	1·04384	1·18401	0·547079	0·850237	0·157198
64 × 64	1·43091	1·04460	1·18908	0·548468	0·858969	0·158858
T3BL(R)						
2 × 2	1·34410	1·06379	1·03872	0·503826	0·678039	0·107921
4 × 4	1·39932	1·04963	1·11324	0·530757	0·747229	0·134221
8 × 8	1·42034	1·04592	1·15618	0·541662	0·802835	0·146709
16 × 16	1·42727	1·04463	1·17613	0·545684	0·834565	0·154149
32 × 32	1·42991	1·04455	1·18513	0·547560	0·851083	0·157317
64 × 64	1·43116	1·04478	1·18937	0·548596	0·859182	0·158891
DRM[7] (16 × 16)	1·4269	1·0436	1·1789	0·5456	0·8435	0·1553
Q4BL[3] (32 × 32)	1·43091	1·04484	1·18685	0·548103	0·851822	0·157164

Morley.[9] For further comparison with Reference 8 Table VI shows the results obtained by the present element and the DRM element[7] in terms of the total strain energy.

4. CONCLUSIONS

A three-node triangular element for the analysis of thick and thin plate bending problems has been presented. The element has three external degrees of freedom at each vertex (a transverse displacement $\bar{w}$ and two rotations $\bar{\theta}_x$ and $\bar{\theta}_y$) and two internal rotational degrees of freedom $\Delta\bar{\theta}$. Moreover, to ensure a higher-order interpolation capacity, the transverse displacement is linked to the rotational degrees of freedoms.

Two forms of the element are discussed: T3BL, in which all integrals, are evaluated exactly, and T3BL(R), in which selectively reduced integration is used. The element was analysed with respect to the mixed patch test, and while it is deficient in meeting a proper rank condition on a single element, it passed the test for meshes of two or more elements as well as all consistency tests.

The two forms of the element perform similarly although the reduced integration form is generally more flexible and approaches the exact values from above.

In closing, we note that the element considered can easily be extended to include non-linear constitutive or large displacement effects. It may also be incorporated into an adaptive mesh strategy using triangles, as proposed by Zienkiewicz and Zhu.[10,11] Thus, the element provides a viable basis for general applications in plates and, when combined with a membrane element, to general shells.

Table V. Displacements and principal moments at the centre of the simply supported (ss1) skew plate under uniform load

Mesh	$L/t = 100$			$L/t = 1000$		
	$W_c \Big/ \left(\frac{qL^4}{100D}\right)$	$-M_1 \Big/ \left(\frac{qL^2}{100}\right)$	$-M_2 \Big/ \left(\frac{qL^2}{100}\right)$	$W_c \Big/ \left(\frac{qL^4}{100D}\right)$	$-M_1 \Big/ \left(\frac{qL^2}{100}\right)$	$-M_2 \Big/ \left(\frac{qL^2}{100}\right)$
T3BL						
2×2	0·537924	0·74946	1·44017	0·537100	0·74915	1·44018
4×4	0·422052	0·95558	1·72438	0·420881	0·95544	1·72257
8×8	0·417401	1·08868	1·89310	0·415286	1·09045	1·89280
16×16	0·417979	1·10714	1·92240	0·413626	1·10028	1·91234
32×32	0·419586	1·12122	1·93657	0·412734	1·09998	1·91781
64×64	0·421447	1·13052	1·94468	0·412062	1·10022	1·91790
T3BL(R)						
2×2	0·732774	0·81994	1·44750	0·731934	0·81964	1·44753
4×4	0·489591	0·96480	1·82077	0·488714	0·96464	1·81994
8×8	0·439706	1·09971	1·91308	0·438700	1·09914	1·91216
16×16	0·427784	1·12719	1·94564	0·426250	1·12484	1·94272
32×32	0·423608	1·13205	1·94739	0·420731	1·12503	1·94017
64×64	0·422851	1·13453	1·94867	0·417437	1·11876	1·93358
Q4BL[3] (mesh 32×32)	0·426951	1·14877	1·96183	0·423520	1·14021	1·95282
Analytic (thin plate) solution	0·4080 (0·423)+	1·08	1·91	0·4080	1·08	1·91

+ Three-dimensional solution by Babuska and Scapolla.[10]

Table VI. Strain energy of the simply supported (ss1) skew plate ($L/t = 100$, uniform load)

Mesh	Strain energy (×10⁴)	
	T3BL	DRM[6]
2×2	0·383241	0·285103
4×4	0·267398	0·256943
8×8	0·261721	0·261289
16×16	0·262122	0·262455
32×32	0·262921	0·262708
64×64	0·263899	
3D solution by Babuska and Scapolla[10]	0·265868	

REFERENCES

1. O. C. Zienkiewicz, Z. Xu, L. F. Zeng, A. Samuelsson and N. E. Wiberg, 'Lined interpolation for Reissner–Mindlin plate elements. Part I: a simple quadrilateral', *Int. j. numer. methods eng.*, **36**, 3043–3056 (1993).
2. Z. Xu, 'A simple and efficient triangular finite element for plate bending', *Acta Mechanica Sinica*, **2**, 185–192 (1986).
3. Z. Xu, 'A thick-thin triangular plate element', *Int. j. numer. methods eng.*, **33**, 963–973 (1992).
4. O. C. Zienkiewicz and R. L. Taylor, *The Finite Element Method, Vol. I*, 4th edn, McGraw-Hill, New York, 1989.
5. O. C. Zienkiewicz and R. L. Taylor, *The Finite Element Method, Vol. II*, 4th edn, McGraw-Hill, New York, 1991.
6. T. J. R. Hughes, *The Finite Element Method—Linear Static and Dynamic Finite Element Analysis*, Prentice Hall, Englewood Cliffs, N.J., 1987.
7. P. Papadopoulos and R. L. Taylor, 'A triangular element based on Reissner–Mindlin plate theory', *Int. j. numer. methods eng.*, **30**, 1029–1049 (1988).
8. I. Babuska and T. Scapolla, 'Benchmark computation and performance evaluation for rhombic plate bending problem', *Int. j. numer. methods eng.*, **28**, 155–179 (1989).
9. L. S. D. Morley, *Skew Plates and Structures, International Series of Monographs in Aeronautics and Astronautics*, Macmillan, New York, 1963.
10. O. C. Zienkiewicz and J. Z. Zhu, 'A simple error estimate and adaptive procedure for practical engineering analysis', *Int. j. numer. methods eng.*, **24**, 337–357 (1987).
11. J. Z. Zhu and O. C. Zienkiewicz, 'Adaptive techniques in the finite element methods', *Commun. Appl. Numer. Methods*, **4**, 197–204 (1988).